Improving the Accuracy of Measurements in Daylit Interior Scenes Using High Dynamic Range Photography

J. Alstan Jakubiec[1], Mehlika Inanici[2], Kevin Van Den Wymelenberg[3], Alen Mahic[3]

[1]Singapore University of Technology and Design, Singapore
[2]University of Washington, Seattle, USA
[3]University of Oregon, Eugene, USA

ABSTRACT: *Measuring the luminous environment enables researchers and practitioners to study perception and visual comfort in existing environments in order to decipher the components that contribute to good or problematic lighting characteristics. High dynamic range photography is commonly used to study visual perception and comfort. This paper presents new findings and specific methods of capturing interior scenes that may include peaks caused by a direct view of the sun and specular reflections. Methods are tested to improve the range of luminance values that can be captured, and new guidelines are proposed to improve the accuracy of computed visual comfort indices.*
Keywords: daylighting, high dynamic range imagery, visual comfort, glare, luminous overflow

INTRODUCTION

Daylighting design is a decision-making process that integrates the outdoor environment, building openings, material properties, lamps, luminaires, and lighting controls. These choices affect visual quality, human comfort, performance, and occupant well-being. Measurement of the luminous environment with affordable technologies such as high dynamic range (HDR) photography paired with relatively inexpensive luminance and illuminance sensors has become a common approach among researchers and practitioners to evaluate visual comfort and perception in this context.

HDR photography (Debevec and Malik, 1997) is a three step technique where: 1) Multiple photographic exposures are captured in the field in a successive manner; 2) they are fused into a single HDR image using computational self-calibration methods; and 3) post-processing is done to account for known aberrations (such as the vignetting effect) and to fine tune the results using a sensor reading taken in the field. Single-aperture HDR photography techniques have been validated for capturing luminance maps of building interiors (Inanici, 2006), and two-aperture and filter-based HDR photography techniques have been successfully used in capturing the sky and simulating image-based lighting for interior and exterior environments (Stumpfel, et al. 2004; Inanici, 2010).

A common use of HDR photography is to evaluate visual comfort in daylit spaces (Fan, et al. 2009; Van Den Wymelenberg, et al. 2010; Konis 2013; Van Den Wymelenberg and Inanici 2014; Konis 2014; Hirning 2014; Van Den Wymelenberg and Inanici 2015; Jakubiec, et al. 2015; Jakubiec, et al. 2016). Being able to accurately measure luminance levels is crucial for the evaluation of existing lighting conditions and for

application in lighting research on topics such as visual comfort, electric lighting or shading controls. However, the authors observe that there are common shortcomings for indoor HDR captures that typically occur when the solar corona or specular reflections are visible in the field of view. When this occurs, typical HDR capture techniques may underestimate the luminance of extremely bright sources that cause discomfort. This inability to measure the full dynamic range of a lighting scene is called luminous overflow. Such shortcomings limit the accuracy of HDR photography in practice; therefore, the intent of this publication is to share important information with the lighting community on missteps in capturing HDR photographs. The paper includes guidelines for measuring bright sources and demonstrates a post-processing method for correcting HDR photographs which exhibit luminous overflow.

In addition, the results of a longitudinal study identifying potential pitfalls from typical HDR capture techniques are presented. Hemispherical HDR photographs were captured with paired vertical illuminance and luminance measurements under a wide variety of lighting conditions, sun positions, and space types. Care was taken to especially include the following conditions: overcast sky, artificial electric illumination, direct vision of the sun, bright specular reflections, intermediate sky, application of shading devices, and combinations of the preceding.

PREVIOUS WORK

This paper is built upon the best practices for HDR image captured laid out in Inanici (2006) and follows from previous work published by the authors (Jakubiec, et al. 2016). In all HDR captures in this paper, full-frame digital cameras outfitted with hemispherical fisheye lenses were used to take HDR photographs. The white

balance of the camera is set to daylight, and ISO sensor sensitivity is set to 100. Luminance measurements of a neutral grey target were measured using a Konica Minolta LS-110 luminance meter. Vertical illuminance measurements were taken at the front of the fisheye lens using a Konica Minolta T-10a illuminance meter. Both illuminance and luminance measurements were repeated before and after the image capture process in order to detect changing lighting levels during the capture.

Inanici (2006) utilized an aperture size of f/4 to capture luminance values within the range of 1–16,000 cd/m². The authors found that this range is not wide enough to include the luminance values around the solar disk which can be as high as a billion cd/m² (Grondzik et al. 2006) nor of intense specular reflections. Much of the authors' previous work therefore related to capturing this high luminance range (Jakubiec, et al. 2016).

Initially, aperture selection was investigated as a factor determining the dynamic range of a HDR photograph. Although any aperture size can be utilized as long as an aperture-specific vignetting correction is applied, the choice impacts both the captured luminance range and potential for lens flare. The authors' found that the expected dynamic range difference between f/4 and f/22 apertures is approximately 32 fold (Jakubiec, et al. 2016), which follows the geometric difference between the two settings. It was also found that the maximum captured luminance is approximately 100,000 cd/m² at f/4 using a Canon EF 8-15mm f/4L USM lens and EOS 5D camera and 3,200,000 cd/m² at f/22 using the same lens and camera. Maximum dynamic range may vary with camera or lens type, and should be checked by researchers. Based on this finding, it stands to reason to use a smaller aperture (such as f/22) to increase the luminance range.

The authors also found that smaller apertures correlated with greater potential for lens flare (Jakubiec, et al. 2016). Lens flare is the result of light scattering in the lens, and it causes false luminance increases around bright light sources. An aperture size of f/11 was chosen as a compromise between increased dynamic range and reduced lens flare, with a maximum luminance range of approximately 850,000 cd/m² while having less potential for lens flare using the aforementioned camera and lens combination.

Since the luminance value of the solar disc is beyond the range a normal HDR can capture using any aperture size, neutral density (ND) filters were investigated to increase the captured range. ND-1, 2, and 3 filters transmit 10%, 1%, and 0.1% of incident light, respectively. A ND-3 filter has been used in capturing HDR images of the sky (Stumpel et al., 2004), but it was not utilized for interior captures. The maximum

luminance capture of a f/11 aperture photograph with a ND-3 filter using the aforementioned example is expected to be approximately 850,000,000 cd/m² (850,000 / 0.001).

It is important to note that ND filters are not truly neutral, and they introduce a chromatic shift that affects the middle luminous ranges substantially. As peak luminances are captured (sun and specular reflections), lower luminances (the rest of the scene) were found to be reduced as compared to a standard capture using Inanici's 2006 method. This effect can be observed in Fig. 1, which illustrates the various capture methods employed in this paper applied to a daylit scene with direct vision of the sun on a clear day. 1A shows the human perception of the scene using the Radiance 'pcond' tool (Ward, 1994), 1B shows a capture without a filter, and 1C shows a capture using a ND-3 filter. The ND-3 filter capture measures a significantly higher solar luminance compared to the normal capture (a nearly 200-factor increase), but it also lowers the average diffuse scene luminance by 33.1% and shifts the color range of the photograph noticeably compared to Fig. 1A.

The authors' previous work also found that the absence of high luminance values due to luminous overflow significantly impacts the calculation of human visual comfort indices such as Daylight Glare Probability (DGP) (Wienold and Christoffersen 2006) and the Unified Glare Rating (UGR) (CIE 1995). UGR values for images corresponding to vertical illuminances greater than 5,000 lx were found to increase on average by a value of 10.17, enough to move an evaluation from 'imperceptible' to 'disturbing.' DGP values for the same images were found to increase on average by 0.23, enough to move an evaluation from 'imperceptible' to 'intolerable.' In most—but not all—cases, vertical illuminances under 5,000 lx indicated a lack of overflow (Jakubiec, et al. 2016). Therefore, the previous study recommended the use of ND filters for conditions above 5,000 vertical lux measured at the camera lens in order to ensure that an adequate luminance range is captured.

METHODOLOGY
Seventy-six HDR photographic series have been captured under a wide variety of interior luminous conditions: overcast skies, intermediate skies, sunny skies, electrically lit, and especially scenes that contain direct vision of the sun or bright specular reflections (those likely to experience luminous overflow and visual discomfort). The vertical illuminances corresponding to the HDR photographs taken range from 25.56 lx–74,850 lx. In order to quantify the effects of luminous overflow, a photograph with no filter (NF) was quickly followed by a photograph with a ND-3 filter. Grey card luminances and vertical illuminances were measured before and after each capture sequence in order to ensure
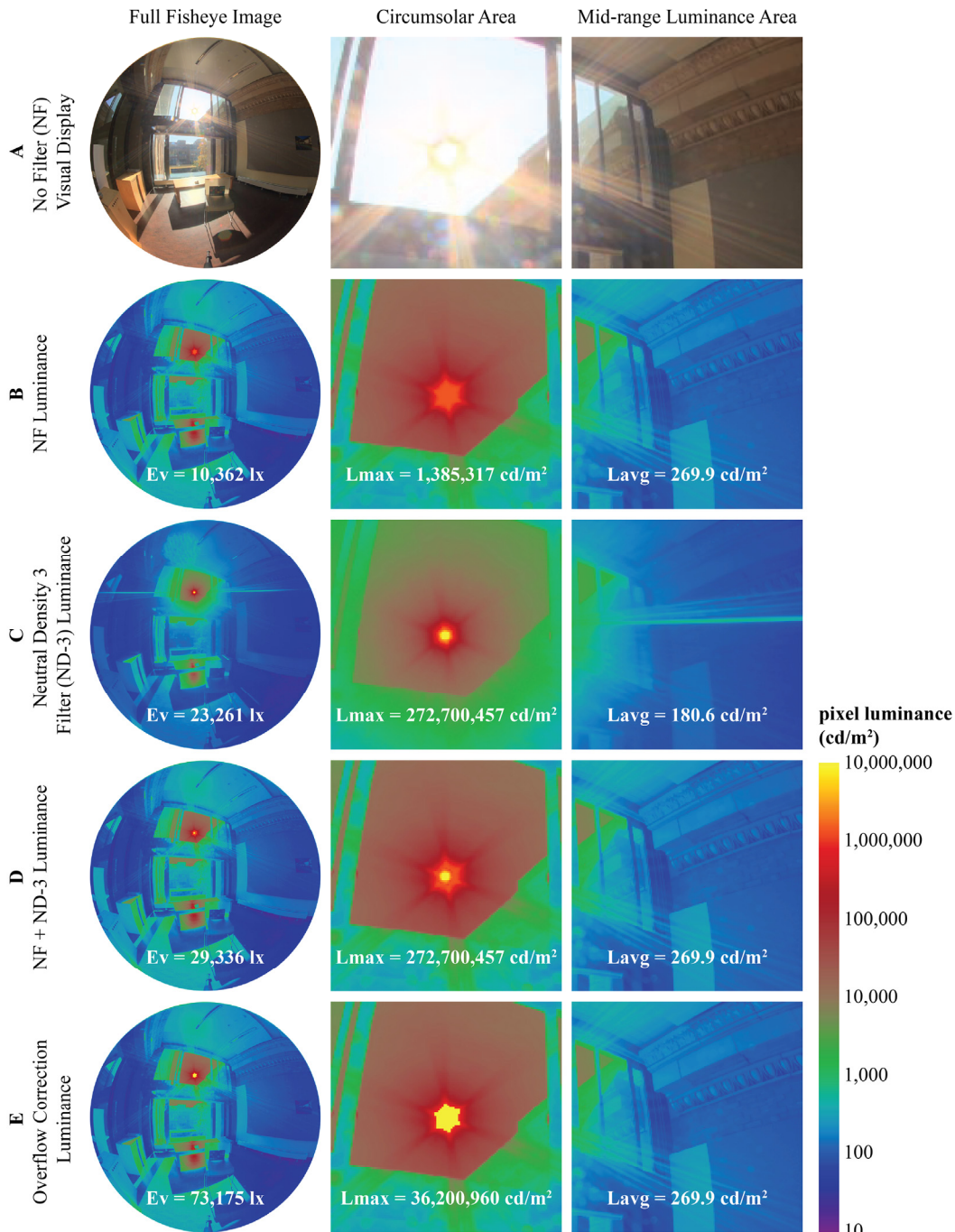
Figure 1:Comparison of image capture and processing techniques explored in this paper

that lighting levels did not change significantly. Large deviations in illuminance, greater than 10%, during a single capture or between the NF and ND-3 captures resulted in images being removed from the study. Therefore all NF and ND-3 HDR images in this study are comparable. All images are corrected for vignetting, when wide angle lenses exhibit noticeable luminance decrease from the centre of the image to the perimeter (Inanici, 2006; Cauwerts and Deneyer 2012, Jakubiec, et al. 2016). Furthermore, each HDR image is calibrated

based on the average of the before-and-after grey card luminance measurements.

It is impossible to know the true luminance of the sun with current technology. The luminance meters available for this study have a maximum range of 999,900 cd/m^2, far short of the billion cd/m^2 potential solar luminance (Grondzik, et al. 2006). Instead, vertical illuminance measurements taken at the lens are used to check the validity of HDR images. These independent illuminance

sensor measurements can then be compared to illuminance calculated from the fisheye image ($E_{v,image}$). This is only possible when a HDR image contains a full hemispherical view, and is calculated as per Equation 1 (following page) as a summation across all pixels in a hemispherical image capture.

$$E_{v,image} = \sum \cos\theta * L * \omega \qquad (1)$$

θ is the incident angle of light arriving at the camera, L is the pixel luminance in cd/m^2, and ω is the solid angle of the pixel in str. Computational methods of calculating illuminance from a hemispherical image using Equation 1 are included in sections A and B of the appendix.

As stated in the previous work section, using a ND-3 filter alone is not fully satisfactory as the mid-range luminances in the scene are reduced. Therefore, two alternative methods are proposed to investigate strong measured luminances while simultaneously maintaining the validity of the rest of the scene luminances. The first method is simply to combine the NF and ND-3 images in an intelligent manner; all pixels in the ND-3 image that are greater than the maximum luminance of the NF image as found using the Radiance 'pextrem' command (Ward 1994, appendix section C) are substituted into the original NF image. Thus, a new image is created where only pixel luminance values above the measurement capacity of the NF image capture are replaced by the more luminous pixels from the ND-3 image. In this way, the more accurate mid-range luminance data of the NF image is maintained while the total luminous range of the image is increased. An example of this process is included in Fig. 1D, where it can be seen that maximum luminance is the same as the ND-3 image but with mid-range luminances identical to the NF image. The strength of this effect is astounding as the image-calculated vertical illuminance increases by 6,075 lx compared the ND-3 image alone. In other words, 6,075 lx of illuminance was lost through the effects of the ND-3 filter on measured mid-range luminance values.

The method described in the previous paragraph is still not ideal, because two HDR photographs need to be taken. This is time consuming, taking up to 2 minutes in the field for an adept user. During those 2 minutes, lighting conditions can change substantially (Jakubiec, et al. 2016). Furthermore the post-processing effort is increased, and the amount of data collection is doubled. An alternative method is to capture only a single image, but increase the luminance of the overflow pixels until the image illuminance is equal to the sensor-measured vertical illuminance. Pixel brightnesses rounded based on the first digit of the NF maximum luminance value are increased until the image illuminance is equal to the measured illuminance. In the case of a photograph of the

direct sun, this spreads out the solar luminance into a larger solid angle area—as shown in Fig. 1E—where the peak luminance is less but covers a larger area. In this paper this post-processing method is referred to as overflow correction. An entire computational procedure for performing luminous overflow correction is documented in the paper appendix.

For each of the four capture methods (NF, ND-3, NF + ND-3, and overflow correction), peak luminances, image-derived illuminances, and visual comfort values—DGP and UGR—are calculated. In this way, it the authors' aim to analyze the phenomena of luminous overflow and make recommendations for its identification and correction.

RESULTS

Fig. 2 (A–D) illustrates comparisons for all 76 image pairs—152 HDR images in total—as a stacked bar chart. In all cases, the colors indicate the capture or correction methodology employed: Dark grey (■) indicates a NF photograph, lighter grey (■) indicates a ND-3 photograph, lightest grey (■) indicates a NF + ND-3 combined photograph, and red (■) indicates an overflow corrected image. The X-axis label value of each bar indicates the mean of 4 vertical illuminance measurements taken at the lens before and after the NF and ND-3 captures. The Y-axis indicates values derived from the images: 2A, peak luminances; 2B, the percentage of sensor-measured illuminance represented by the photograph; 2C, image-derived DGP visual comfort values; and 2D, image-derived UGR visual comfort values.

Fig. 2B illustrates that most images under 5,000 vertical lux do not experience overflow, as they are close to the sensor-measured lux value; on average 88.6% of sensor-measured illuminance is represented by images where $E_v < 5,000$ lx. On the other hand, images above 5,000 vertical lux are highly likely to experience overflow. On average only 28.6% of illuminance is represented in a NF photograph for scenes where $E_v \geq 5,000$ lx. Using a ND-3 filter increases the mean percentage of measured illuminance to 48.0% even though the mid-range luminances are attenuated. Using the NF + ND-3 combined image, on average 54.5% of measured illuminance is represented by the HDR image. These results suggest that for many high-illuminance situations, $\geq 5,000$ lx, the direct solar component is dominant, representing on average 71.6% of the total visible light present in such scenes. It is also noteworthy that even with a dynamic range of between 10^8–10^9 cd/m^2 (2A) for most extremely high illuminances (>25,000 lx), the NF + ND-3 images cannot come close to representing the incident illuminance.
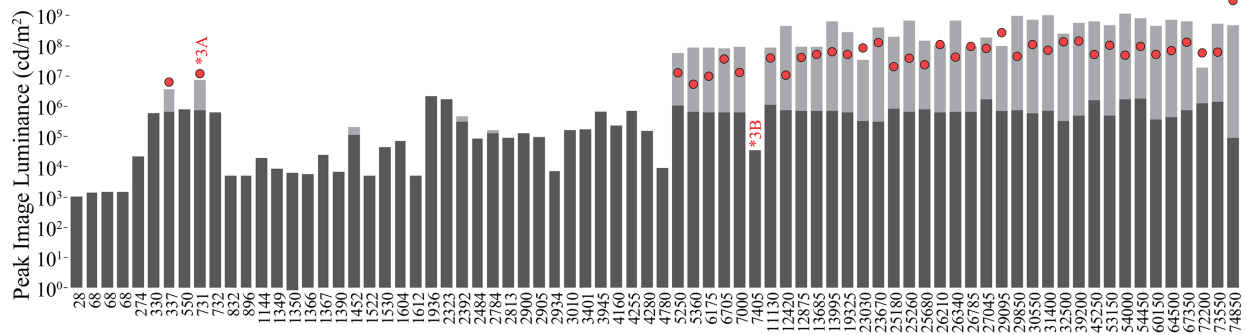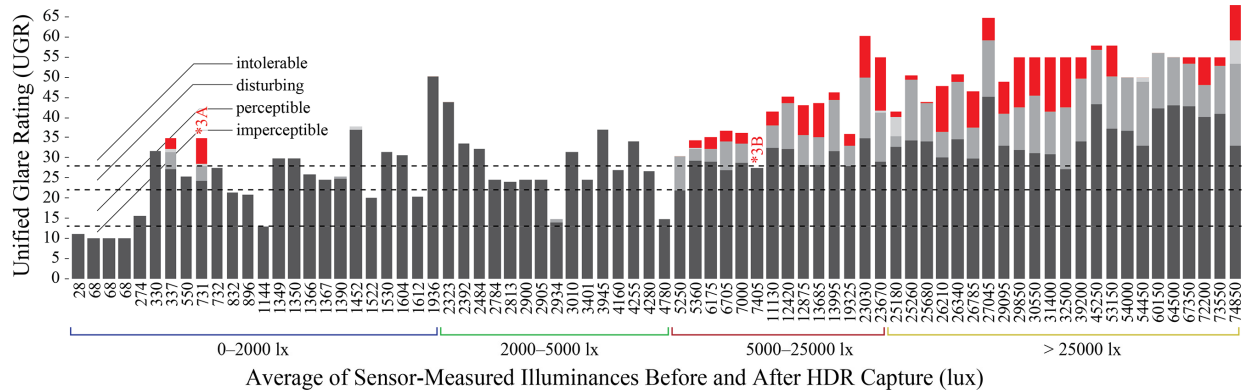
A. Comparison of Peak Image Luminance
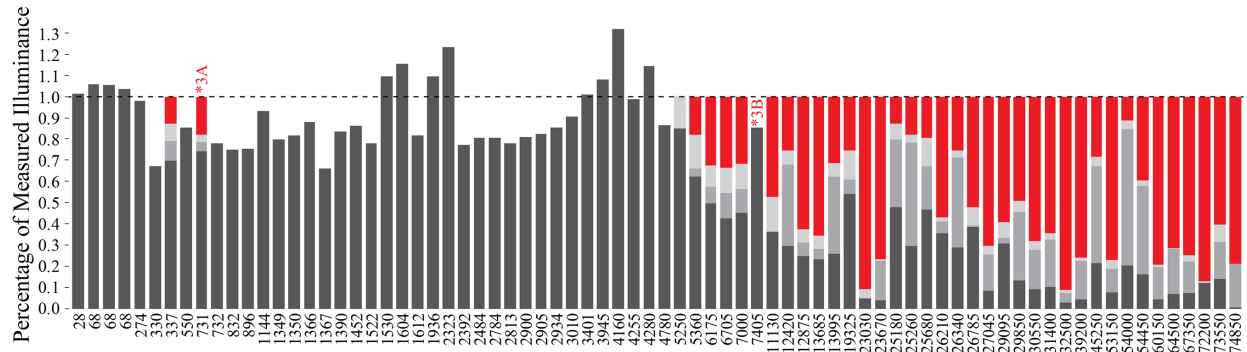
B. Comparison of the Percentage of Measured Illuminance Resolved by HDR Images
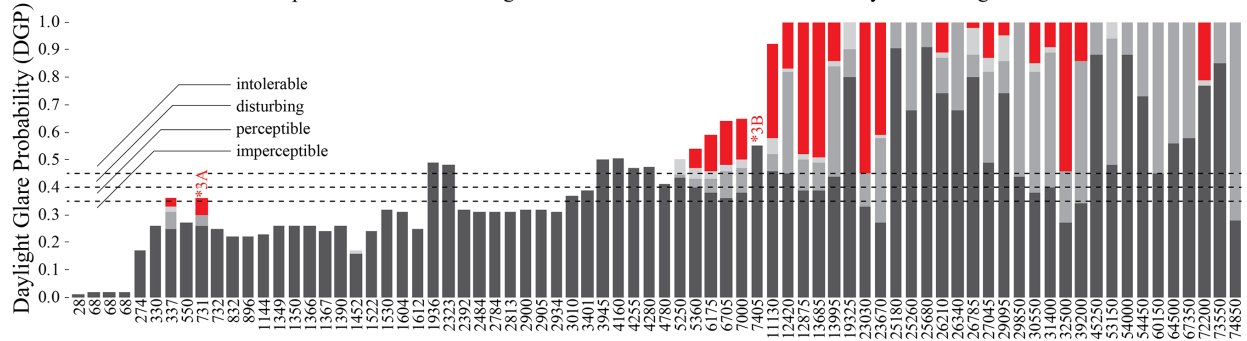
C. Comparison of Image-derived DGP Values

D. Comparison of Image-derived UGR Values

Figure 2:Comparison of image capture and processing techniques explored in this paper

Expanding the dynamic range of photographs to the extent seen so far in this paper does not fully represent the sensor-measured illuminance. This suggests that further dynamic range is needed such as by applying a ND-4 filter (0.01% of light transmitted) or using a f/22 aperture, or that measurements of luminance are not vary accurate at such high values. However, a ND-4 filter is exceedingly difficult to use indoors as it is nearly impossible to get a proper exposure, and it is likely to further reduce mid-range luminances. Choosing a f/22 aperture increases the risk of lens flare as previously mentioned. Therefore, correcting for overflow using the NF photograph and measured vertical illuminance as previously described and depicted in Fig. 1E is a plausible option.

Overflow correction achieves photometric parity ($E_v = E_{v,image}$) by virtue of its method of adjusting the image until it equals the measured illuminance. A valid concern with overflow correction is whether it may give inaccurate results in terms of glare metrics such as DGP and UGR. Figs. 2C and 2D begin to address this concern, comparing the metrics for the four capture and correction methods. It is often the case that overflow correction increases glare metric results, especially for aforementioned vertical illuminance conditions greater than 5,000 lx. However, the real question is if the evaluation of the metric changes with the overflow correction. For DGP results, only two images (at 337 and 731 lx E_v) are moved from one subjective threshold to another beyond the value of the NF + ND-3 method. For UGR results, no single image was changed from one subjective threshold to another.

CONCLUSION AND DISCUSSION

It is likely acceptable to identify luminous overflow conditions from an illuminance mismatch between HDR photographic illuminance and a sensor measurement. It is plausible to correct for the overflow using the measured illuminance value without taking a second photograph with a wider range of luminance capture. The authors found that the overflow correction method proposed herein generates similar results when considering the subjective evaluation of the visual comfort metrics DGP and UGR as well as peak image luminances. In order to ensure the accuracy of HDR images against luminous overflow, the authors make several new recommendations:

1. Measure the luminous range of the specific camera, lens, ISO, and shutter speed combinations to be used in any measurement by capturing a very bright source such as the sun or a halogen lamp. The peak luminance of this image is near the value at which overflow will occur using the specific hardware and camera settings.
2. Measure vertical illuminance in addition to luminance with every HDR photograph. Illuminance

derived from the resulting HDR image should be comparable to the sensor measurement if the image is accurately representing luminances in the scene.
3. When the peak luminance of any given HDR image is near the maximum luminous range of the image and the image-computed vertical illuminance is below the sensor measured value, the image likely exhibits luminous overflow. These images should be corrected for the overflow condition or discarded.

Another observation from this study is that luminous overflow is more likely to occur at vertical illuminances greater than 5,000 lx; however, that is not deterministic as seen in Fig. 3A and labeled in Fig. 2 with *3A where overflow occurs through a fabric roller shade at only 731 lx. Likewise, overflow does not always occur for high illuminance images as seen in 3B illustrating a large visible solid angle of diffuse sky at 7,405 lx (labeled *3B in Fig. 2). These observations are important to keep in mind when using automated capture methods during long-term visual comfort studies.

It is observable from Figs. 2C and 2D that DGP as a metric is highly sensitive to overflow. Twenty image pairs of 38 that exhibit overflow (52.6% of overflow images) move the DGP value from one subjective threshold using a NF capture to another higher discomfort threshold. Conversely, this only occurs for 4 of the same 38 images (10.5%) for the UGR metric. Therefore, UGR is more likely to evaluate 'as intended' even when luminous overflow is observable.

The time and monetary cost of verifying the accuracy of HDR photographs and ensuring against luminous overflow is relatively small. Using Inanici's (2006) capture method, it is recommended to always use an independent luminance measurement of a grey card. To perform measures before and after a HDR capture and to add in a vertical illuminance measurement as recommended in this paper is a relatively small time contribution for the photographer. A high-quality illuminance sensor costs roughly 1/8 as much as an equivalent quality luminance sensor, so the monetary cost is also low. If a photographer is not using independent sensor measurements with each HDR capture, then the monetary barrier is high (a $6,000–$10,000 investment), but the user should realize that the uncertainty of the results are significantly increased without a measurement-based calibration. The analysis and correction process can either be done manually or with automated analysis scripts (as described in the appendix). This requires users to be organized with their data. The analysis and correction process is very fast, on the order of seconds, relative to glare evaluation programs such as Evalglare (Wienold 2015) and the time required to capture and analyze the input images.
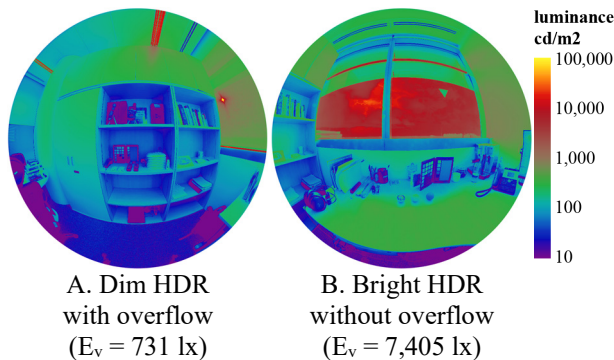
A. Dim HDR
with overflow
(E_v = 731 lx)

B. Bright HDR
without overflow
(E_v = 7,405 lx)

Figure 3: Example HDR images of atypical luminous overflow (or lack thereof) cases

Further work is necessary in order to validate the simple illuminance-based correction for luminous overflow proposed in this paper. Specifically, it may be more accurate to place all of the 'overflow' luminous energy into a pixel source roughly the size of the solar disc centered within the overflow pixels rather than adjusting all of the overflow pixels to be more luminous. The validation and study of such other corrective methods is the subject of future work for the authors.

ACKNOWLEDGEMENTS

REFERENCES

CIE,1995. CIE 117-1995. *Discomfort Glare in Interior Lighting*. Vienna: CIE.

Cauwerts, C., and A. Deneyer, 2012. Comparison of the Vignetting Effects of Two Identical Fisheye Lenses. *Leukos*, 8(3), pp.181-203.

Debevec P. and J. Malik, (1997). Recovering high dynamic range radiance maps from photographs. In *SIGGRAPH Computer Graphics Proceedings*, Los Angeles, CA, pp.369-378.

Fan, D., B. Painter and J. Mardaljevic, 2009. A Data Collection Method for Long-Term Field Studies of Visual Comfort in Real-World Daylit Office Environments. In Proc. of PLEA (pp. 251-256).

Grondzik, W.T,. A.G. Kwok, B. Stein and J.S. Reynolds, 2006. Mechanical and Electrical Equipment for Buildings. John Wiley & Sons.

Hirning, M.B., G.L. Isoardi and I. Cowling, 2014. Discomfort Glare in Open Plan Green Buildings. Energy and Buildings, 70, pp.427-440.

Inanici, M., 2006. Evaluation of high dynamic range photography as a luminance data acquisition system. *Lighting Research and Technology*, 38(2), pp.123-134.

Inanici, M., 2010. Evalution of High Dynamic Range Image-Based Sky Models in Lighting Simulation. *Leukos*, 7(2), pp.69-84.

Jakubiec, J.A., C. Reinhart and K. Van Den Wymelemberg, 2015. Towards an Integrated Framework for Predicting Visual Comfort Conditions from Luminance-Based Metrics in Perimeter Daylit Spaces. In *Proc. of Building Simulation*. Hyderabad, India, Dec. 7-9.

Jakubiec, J.A., K. Van Den Wymelenberg, M. Inanici, and A. Mahic, 2016. Accurate Measurement of Daylit Interior Scenes Using High Dynamic Range Photography. In *Proc. of CIE Conference on Lighting Quality and Energy Efficiency*. Melbourne, Australia.

Konis, K., 2014. Predicting Visual Comfort in Side-lit Open-Plan Core Zones: Results of a Field Study Pairing High Dynamic Range Images with Subjective Responses. *Energy and Buildings*, 77, pp.67-79.

Stumpfel J., A. Jones, A. Wenger and P. Debevec, (2004). Direct HDR capture of the sun and sky. In *3rd International Conference on Virtual Reality, Computer Graphics, Visualization and Interaction in Africa*. Cape Town, South Africa.

Van Den Wymelenberg, K., M. Inanici and P. Johnson, (2010). The Effect of Luminance Distribution Patterns on Occupant Preference in a Daylit Office Environment. *Leukos*, 7(2), pp.103-122.

Van Den Wymelenberg, K. and M. Inanici, (2014). A Critical Investigation of Common Lighting Design Metrics for Predicting Human Visual Comfort in Offices with Daylight. Leukos, 10(3), pp.145-164.

Van Den Wymelenberg, K. and M. Inanici, (2014). Evaluating a New Suite of Luminance-Based Design Metrics for Predicting Human Visual Comfort in Offices with Daylight," *Leukos*, DOI: 10.1080/15502724.2015.1062392.

Ward, G., (1994). The Radiance Lighting Simulation and Rendering System. In *Proceedings of SIGGRAPH 94, Computer Graphics Proceedings*, Annual Conference Series, pp. 459-572.

Ward, G.J. Photosphere, Computer software, [Online], Available: <http://www.anyhere.com/>. [26 February 2016].

Wienold, J. and J. Christoffersen, (2006). Evaluation methods and development of a new glare prediction model for daylight environments with the use of CCD Cameras. *Energy and Buildings*, 38(7), pp.743-757.

Wienold, J. Evalglare 1.17, computer software 2015. Available from: <https://github.com/NREL/Radiance/>. [15 October 2015].

APPENDIX: OVERFLOW CORRECTION

The process of correcting a HDR image for overflow is described in greater detail within this appendix. Specific command line functions are illustrated using the Radiance suite of tools (Ward 1994). This process was automated using a simple script for the presented research.

A. Masking a HDR Image

A monochromatic bitmap format image of a white circle and a black background with the same dimensions as the HDR photograph can be converted to the Radiance RGBE format using the below command,

```
ra_bmp -r mask.bmp > mask.hdr
```

And HDR images can have this mask applied by the following command,

```
pcomb -e "lo=mask * li(1); mask=if(li(2)-.1,1,0);"
    -o image.hdr -o mask.hdr > image_masked.hdr
```

It is necessary to append the original view information to the resulting file header as the 'pcomb' command comments the information out of the image header. In the case of a typical hemispherical fisheye image, this is,

```
VIEW= -vta -vh 180 -vv 180
```

B. Calculating Illuminance from a Masked Image

Illuminance can be calculated from a circularly masked hemispherical fisheye image (as created in A) using the command,

```
pcomb -e "lo=L * Sang * cosCor; L=179 * li(1);
    Sang=S(1); cosCor=Dy(1);" -o image_masked.hdr
    | pvalue -d -b -h -H
    | total
```

C. Finding the Maximum Pixel Luminance

The Radiance command,

```
pextrem image.hdr
```

will return the location and RGB Radiance values of the extreme brightest and darkest pixels. The luminance of these pixels can be determined by Equation 2 using a standard 179 lm/W conversion factor in Radiance.

$$L = 179 * (0.2651R + 0.6701G + 0.0648B) \quad (2)$$

D. Determining the Solid Angle of Pixels Above a Set Luminance Threshold

The solid angle size of pixels over a set luminance threshold (less than a factor of L, $L_{threshold}$) can be determined using,

```
pcomb -e "lo=if(li(1)-L_threshold/179, Sang, 0);
    Sang=S(1);" -o image_masked.hdr
    | pvalue -d -b -h -H
    | total
```

E. Increasing Overflow Pixel Luminances to Achieve a New Illuminance Value

In order to increase pixels over a certain luminance to match an image's calculated illuminance ($E_{v,image}$) to an illuminance measurement (E_v), first the current illuminance contribution ($E_{contrib}$) of the pixels to be corrected should be determined using the command,

```
pcomb -e "lo=if(li(1)-L_threshold/179,
    illContrib, 0); illContrib=L*Sang*cosCor;
    L=179*li(1); Sang=S(1); cosCor=Dy(1);"
    -o image_masked.hdr
    | pvalue -d -b -h -H
    | total
```

And the potential contribution factor ($C_{potential}$) of the same group of overflow pixels is the sum of the solid angle and cosine correction for each pixel. This can be determined by the following,

```
pcomb -e "lo=if(li(1)-L_threshold/179, illPoten,
    0); illPoten=Sang*cosCor; Sang=S(1);
    cosCor=Dy(1);" -o image_masked.hdr
    | pvalue -d -b -h -H
    | total
```

It is then possible to select a new pixel luminance to make the $E_{v,image}$ equal to the measured value of E_v as in Equation 3 below,

$$L_{new} = \frac{E_v - \left(E_{v,image} - E_{contrib}\right)}{C_{potential}} \quad (3)$$

And finally this new luminance value (L_{new}) can be used to replace pixels over the luminance threshold,

```
pcomb -e "lo=if(li(1)-L_threshold/179, L_new/179,
    li(1));" -o image_masked.hdr >
    image_corrected.hdr
```

It is again necessary to append the original view information to the resulting file header. In the case of a hemispherical fisheye image, this is,

```
VIEW= -vta -vh 180 -vv 180
```